CHAPTER III

REVIEW LITERATURE

3.1 Existing Methods for Reducing pulse width of 3D RF Pulse

To overcome the limitation of the 3D RF pulse length, the 3D pulses can be subdivided into several shots. Each shot is used to separate excitation and acquisition which is called multi-shot [22]. The other technique, a 3D variable-density spiral method by Stenger et.al., MRM, 34:388-394, 1995 [8] can reduce the pulse duration due to decrease sampling at high frequency.

According to long pulse duration of the 3D RF, many authors have purposed an alternative 2D spatially-selective excitation. Lei Zhao *et.al.*[23] combined 2D spatially-selective excitation and the Unaliasing by Fourier-encoding the Overlaps the temporal dimension (UNFOLD) technique. Saritas *et. al.*[4] and Susanne *et. al.*[24] used 2D spatially selective echo planar RF pulse with single-shot EPI acquisition. Finsterbusch *et. al*.[25] used 2D selective excitation for line scan imaging.

3.1.1 Multi-shot 3D Slice-Select Tailored RF Pulses

The multi-shot 3D spiral stack tailored RF pulse exploits the linearity of the small tip angle approximation [26] by breaking up the pulse into orthogonal components that excite the slice or slab in separate acquisition. The final image is obtained by summing the magnitude of each image. The multi-shot method adapted and extended from 2D pinwheels, demonstrated by CJ Hardy using these pulse for 31-Phosphorus NMR excitation pulses[10], to 3D pinwheels by A. Stenger *et.al.*[22]. Two types of multi-shot 3D TRF are consist of stack spiral and skip k_z methods.

3.1.1.1 Stacked spiral k-space

The stacked spiral k-space is one of the fastest known trajectories through 3D k-space [6].The trajectory is created from 2D spiral trajectories in k_x-k_y and gradient "blip" along k_z such that a cylindrical k-space volume is covered. The 2D spiral trajectories design uses the analytical algorithm by Glover [17]. In creating this algorithm, Glover modified the slew rate limited algorithm of Duyn and Yang [27]. This algorithm includes a modified slew rate-limited case for the trajectories near origin and switches to an amplitude-limited case when maximum allowed gradient is being reached. The 2D spiral k-space can also split into several interleaves for multi-shot excitation as show in figure 3.1
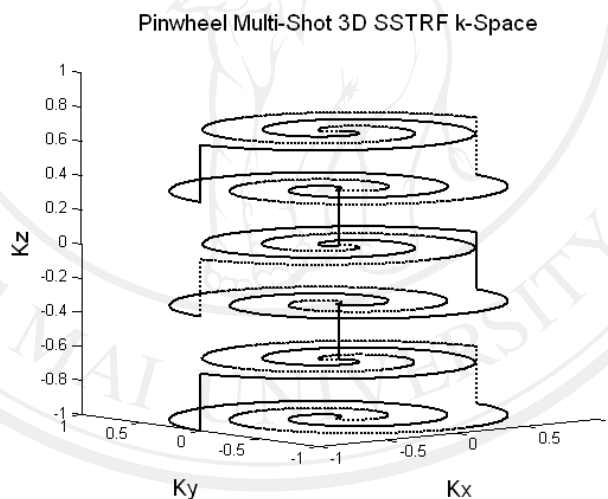
Figure 3.1 Diagrams of the k-space trajectories used for the stack (alternating in-out) spiral of multi-shot 3D RF pulse designs.

3.1.1.2 Skip k_z method

Stenger, *et.al* [5, 8, 22] presented this method for application of multishot 3D slice selective tailored RF pulses for MRI. In brief, full k-space has performed in k_x-k_y plane, and skip spiral slices along k_z direction for reduce pulse duration per shots. This

design is not appropriate for our work due to insufficient sampling in k_z direction.

Figure 3.2 show the skip k_z of two shots 3D slice selective tailored RF pulse designs.
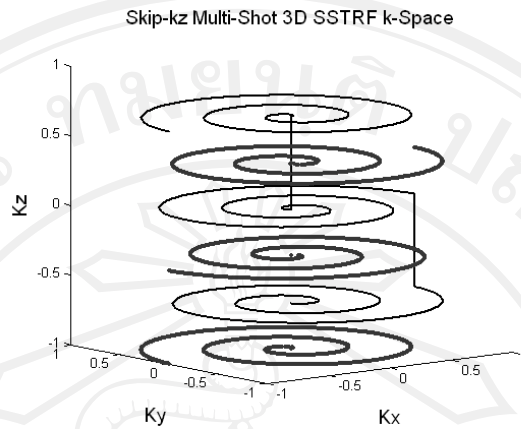
Figure 3.2 Diagrams of the k-space trajectories used for skip-k_z multi-shot 3D RF pulse designs. First shot is bold line and second shot is thin line.

3.1.2 Variable-Density Spiral

The variable-density spiral excitation k-space trajectory is comparable to that used for acquisitions [8].The k-space predominantly at low spatial frequency or center of k-space. Variable-density is sampling in the center uniformly, and the edges reduced density, the result can trade pulse length for a small increasing aliasing of the slice profile [8]. The variable-density trajectory can be used in multi-shot 3D TRF pulses design for reduce pulse duration [8].
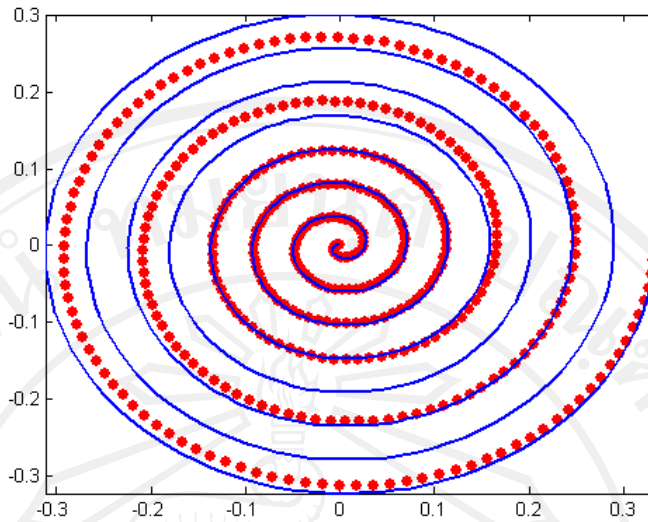
Figure 3.3 diagram of constant-density (solid line) and variable density factor 1.9 (dash line) spiral k-trajectories

3.1.3 Fast K_z TRF

The fast k-z 3D TRF pulse traverses k-space along z rapidly with several slice-select sub-pulses and blip along x-y direction [9]. This pulse provides a pulse width down to less than 5 ms. However, it can not be applied for a thick slice.

3.1.3 2D spatially selective RF excitation

The concept of this method is to actively excite only the parts of the volume that will be used for imaging which is called reduced FOV imaging. The 2D echo planar RF is preferred to use [4, 23, 24]. The pulse duration is the expense of thin slice select, such as 18 ms of 2D echo-planar RF pulse that is designed for 4 mm. of slice thickness [4].

3.2 Proposed Method

This work proposes a new concept of shortening pulse length of the 3D RF pulse in three dimensions (x-y and z) by splitting the 3D TRF pulse in x-y plane as of the previous multi-shot 3D TRF pulse design [22] then each shot along x-y plane is weighted with a half sinc pulse similar to that of the half pulse design.

3.2.1 A Design of Multi-shot Three Dimensional RF pulses (3D RF)

The multi-shot 3D tailored RF pulse as proposed by Stenger et al. [5, 22] was modified as a part of our new 3D RF pulse. The pulse comprises of two major parts, weighting function and a stack-of-spiral k-space trajectory. The weighting function was designed in spatial domain and exploiting small tip angle approximation by taking the Fourier transform of the design function to obtain B_1 waveform. For the stack of spirals k-space trajectory, constant sampling density spirals was designed using analytical technique of Glover. The multi-shot method exploits the linearity of the small tip excitation by breaking up the pulses into two orthogonal components that excite the slice in separate acquisition, as shown in figure 3.4.
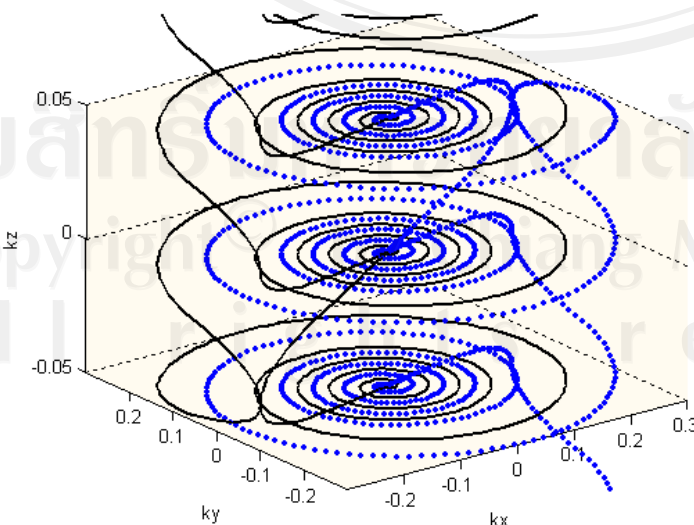
Figure 3.4 Show two shots of spiral k-trajectories outward, first shot is dot line and second shot is solid line.

3.2.2 Half-pulse design along k_z direction

The half-pulse was applied in the slice select direction of the new 3D RF pulse. The two half-sinc RF excitation pulses was implemented by breaking up a window-Sinc pulses into 2 half-pulses, and each half pulse will excite and acquire separately. The half-sinc pulse is inherently self-refocused and will be applied during the rising and falling slopes of the slice-selection gradient. Mathematical explanation is discussed as below. Prior to understanding the derivation of the half-pulse excitation, a small tip angle approximation needs to be mentioned.

Base on the small tip angle approximation, the transverse magnetization, $M_{xy}(r,t)$ is the Fourier transform of a spatial frequency weighting function W($\mathbf{k}$) multiplied by spatial frequency sampling function S($\mathbf{k}$) as shown in Eq.(3.1).

$$M_{xy}(\mathbf{r},t) = iM_0 \int_k W(\mathbf{k})S(\mathbf{k})e^{i2\pi \mathbf{k}\cdot \mathbf{r}}d\mathbf{k} \tag{3.1}$$

The Eq.(3.1) implies that we can predict slice profile of the transverse magnetization by the Fourier transform of W(k)S(k). W(k) can be solved by the Fourier transform of $M_{xy}(r)$ or the desired shape for excitation.

$$M_{xy}(\mathbf{r}) = i\gamma M_0 \int_0^T \mathbf{B}_1(t)e^{i\mathbf{r}\cdot\mathbf{k}(t)}dt \tag{3.2}$$

where

$$\mathbf{k}(t) = -\gamma \int_t^T \mathbf{G}(s)ds \tag{3.3}$$

$$B_1(t) = -\Delta(k(t))|\gamma G(t)|W(k(t)) \tag{3.4}$$

where $\Delta(k(t))$ is the inverse sample density of k-space trajectory. We modified outward spiral k-space with sampling density weighting function similar to that of the inward spiral k-space proposed by C J Hardy *et.al* [3];

$$1/\rho(k(t)) = (k_{max}/n)\frac{\omega(t/T)}{\sqrt{\omega^2(t/T)^2+1}} \tag{3.5}$$

Where n is the number of spiral turns, $\omega = 2\pi n/T$ and T is pulse duration

G(t) is the gradients simultaneously with RF or $B_1(t)$. From the Eq.3.2, the magnetization along x-y plane can be estimated from the Fourier transform of B_1 and vice versa. If we focus on the M_{xy} at particular z, M_{xy} or slice profile becomes a function of z, $M_{xy}(z)$ and the slice profile $M_{xy}(z)$ is proportional to the Fourier transform of the $B_1(t)$ according to the small tip angle approximation. The full conventional pulse $B_1(t)$ can be further split into two half-pulses, $B_1^+(t)$ and $B_1^-(t)$ as on equation (3.6)

$$M_{xy}(z) = \Im\{B_1^+(t) + B_1^-(t)\} \tag{3.6}$$

The $B_1^+(t)$ can be written as

$$\begin{aligned}
B_1^+(t) &= B_1(t)u(t) \\
\Im(B_1^+(t)) &= B_1(k) \otimes U(k) \\
&= B_1(k) \otimes \left[\frac{1}{2}\delta(k) - i\frac{1}{2\pi k}\right] \\
&= \frac{1}{2}\left[B_1(k) + i\{B_1(k) \otimes (-\frac{1}{\pi k})\}\right]
\end{aligned} \tag{3.7}$$

Likewise, for the $B_1^-(t)$

$$\Im\{B_1^-(t)\} = \frac{1}{2}\left[B_1(k) - i\{B_1(k) \otimes (-\frac{1}{\pi k})\}\right] \tag{3.8}$$

The two half excitations are combined, given that

$$B_1(t) = B_1^+(t) + B_1^-(t) \tag{3.9}$$

With the linearity of the Fourier transform equation (3.9) becomes

$$B_1^+(k) + B_1^-(k) = B_1(k) \tag{3.10}$$

Substitute Eq. 3.7 and 3.8 into Eq. 3.6 obtaining

$$M_{xy}(z) = \frac{1}{2}\big[2 \cdot B_1(t)\big] \tag{3.11}$$

The desired slice profile M_{xy} is added and the imaginary or antisymmetric parts from

Eq. 3.7 and Eq. 3.8 are canceled out, as shown in figure 3.5
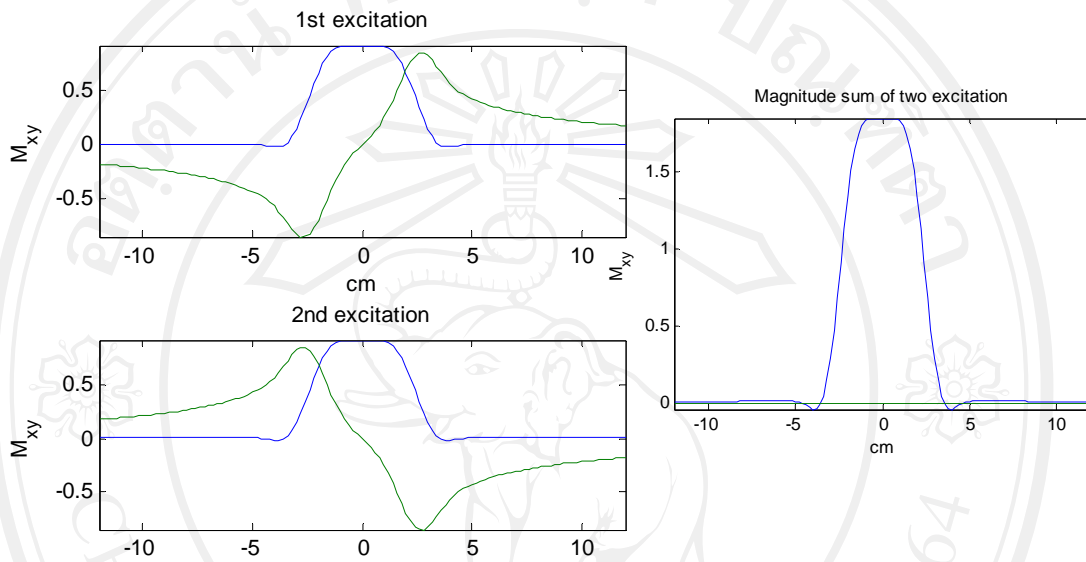
Figure 3.5 Half-window sinc pulse slice profiles obtained by Bloch equation simulation

(top and bottom left) the profiles from two successive excitations with opposite polarity of the slice select.(right) the effective profile of magnitude sum, M_x components cancel and are not observed while M_y components add to produce the desired slice profile.